

UNCLASSIFIED

AD NUMBER
AD479430
NEW LIMITATION CHANGE
TO Approved for public release, distribution unlimited
FROM Distribution authorized to U.S. Gov't. agencies and their contractors; Critical Technology; OCT 1965. Other requests shall be referred to Commanding Officer, U.S. Army Materiel Command, Attn: AMCMU-IS, Washington, DC.
AUTHORITY
USAARADCOM ltr, 20 Feb 1981

THIS PAGE IS UNCLASSIFIED

19
BRL R 1302

BRL

AD

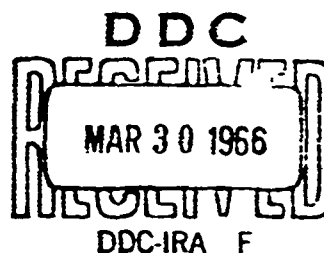
REPORT NO. 1302

LIQUID FILLED GYROSCOPE:
THE EFFECT OF REYNOLDS NUMBER ON RESONANCE

by

B. G. Karpov

October 1965



This document is subject to special export controls and each transmittal to foreign governments or foreign nationals may be made only with prior approval of U.S. Army Materiel Command, Attn: AMCMU-IS, Washington, D.C.

U. S. ARMY MATERIEL COMMAND
BALLISTIC RESEARCH LABORATORIES
ABERDEEN PROVING GROUND, MARYLAND

Destroy this report when it is no longer needed.
Do not return it to the originator.

The findings in this report are not to be construed as
an official Department of the Army position, unless
so designated by other authorized documents.

BALLISTIC RESEARCH LABORATORIES

REPORT NO. 1302

OCTOBER 1965

LIQUID FILLED GYROSCOPE:
THE EFFECT OF REYNOLDS NUMBER ON RESONANCE

B. G. Karpov

Exterior Ballistics Laboratory

This document is subject to special export controls and each transmittal to foreign governments or foreign nationals may be made only with prior approval of U.S. Army Materiel Command, Attn: AMCMU-IS, Washington, D.C.

RDT&E Project No. 1P014501A33D

ABERDEEN PROVING GROUND, MARYLAND

Previous page was blank, therefore not filmed.

BALLISTIC RESEARCH LABORATORIES

REPORT NO. 1302

BGKarpov/blw
Aberdeen Proving Ground, Md.
October 1965

LIQUID FILLED GYROSCOPE:
THE EFFECT OF REYNOLDS NUMBER ON RESONANCE

ABSTRACT

A gyroscope with frictionless bearings was designed and built. Resonance experiments with oils of various viscosities substantiated the results of the author's previous work, i.e., to account for the observed behavior of the gyroscope at resonance, Stewartson's inviscid theory^{2*} requires a viscous correction. Wedemeyer's³ theory for viscous correction predicts that, for a laminar boundary layer on the walls of the cavity, the damping factor should be of the form

$$\delta = \frac{\text{constant}}{\sqrt{\text{Re}}} .$$

This has been verified by present experiments.

The experiments also showed that the rate of growth of the nutational amplitude at resonance is strongly influenced by the nature of the boundary layer. At larger amplitudes, non-linear behavior of the oscillating fluid appears to dominate responses of the gyroscope.

* *Superscript numbers refer to references which may be found on page 36.*

Previous page was blank, therefore not filmed.

TABLE OF CONTENTS

	Page
ABSTRACT.	3
1. INTRODUCTION.	7
2. THE GYROSCOPE	9
3. THE EXPERIMENTS	12
4. THE DATA.	13
5. DAMPING FACTORS	14
6. THE AMPLITUDES.	18
7. FREQUENCY DISPLACEMENT.	32
8. CONCLUDING REMARKS.	34
REFERENCES.	36
DISTRIBUTION LIST	37

1. INTRODUCTION

Experiments¹ performed with liquid-filled shell in free flight and with a liquid-filled gyroscope have shown that the dynamic response of these systems at resonance (instability) is Reynolds number dependent. In comparison with Stewartson's inviscid theory², it was found that at lower Reynolds numbers:

- a. The rate of divergence of the nutational amplitude at resonance is not as large as predicted.
- b. The resonance band is considerably broader than predicted.
- c. The resonance occurs at a slightly lower frequency than the nutational frequency of the system.

Agreement with the inviscid theory improves as Reynolds numbers increase, and at Reynolds numbers of the order of 10^6 , the agreement should be very good.

Wedemeyer has shown³, that these differences between inviscid theory and observations with real fluids can be reconciled by postulating the existence of a boundary layer on the walls of the cavity. The boundary layer arises as a consequence of interaction between the perturbation velocities in the rotating fluid and the walls of the cavity. Fluid energy is lost in this interaction and an effective damping is introduced into the oscillating fluid. All fluid frequencies, therefore, instead of being pure imaginaries, as in inviscid theory, would be complex quantities. In Stewartson's notation, these would be of the form

$$\tau_o = \tau_{oo} + i\delta ,$$

where τ_{oo} is the resonant frequency of an inviscid fluid and δ is the damping factor of the τ_o mode. Wedemeyer also has shown that for a laminar boundary layer the damping factor should be of the form

$$\delta = \frac{\text{constant}}{\sqrt{Re}}$$

where Re is the Reynolds number defined as

$$Re = \frac{\omega a^2}{\nu}$$

with ω axial spin
 a radius of the cavity
 ν kinematic viscosity.

However, in the experiments reported in Reference 1, it was found that the experimental data are better represented by the damping factor:

$$\delta = \frac{\text{constant}}{\sqrt[4]{Re}} .$$

The reason for the $-1/4$ power dependence on Reynolds number rather than $-1/2$ was not clear. It was pointed out, however, that although the range of the Reynolds numbers of the experiments was fairly large, their distribution was such that the exponent of Re in correlation of δ vs Re could not be well determined.

There was another element which could have contributed to the $-1/4$ power dependence of δ on Re. The outer and inner gimbals of the gyroscope were supported by ball-bearings. These bearings showed strongly non-linear damping behavior at small amplitudes. Hence, all measurements of the damping rates were made at fairly large amplitudes, between one and five degrees. It was conjectured that even if a laminar boundary layer existed at very small oscillations, it could become unstable at larger amplitudes. This might have led to a different power dependence on the Reynolds numbers.

To resolve this matter, and for other reasons, a gyroscope of greater sensitivity was required. Such a gyroscope was designed and built.

The previous resonance experiments were repeated with considerably better distribution of Reynolds numbers. The results of these experiments are the subject of this report.

2. THE GYROSCOPE

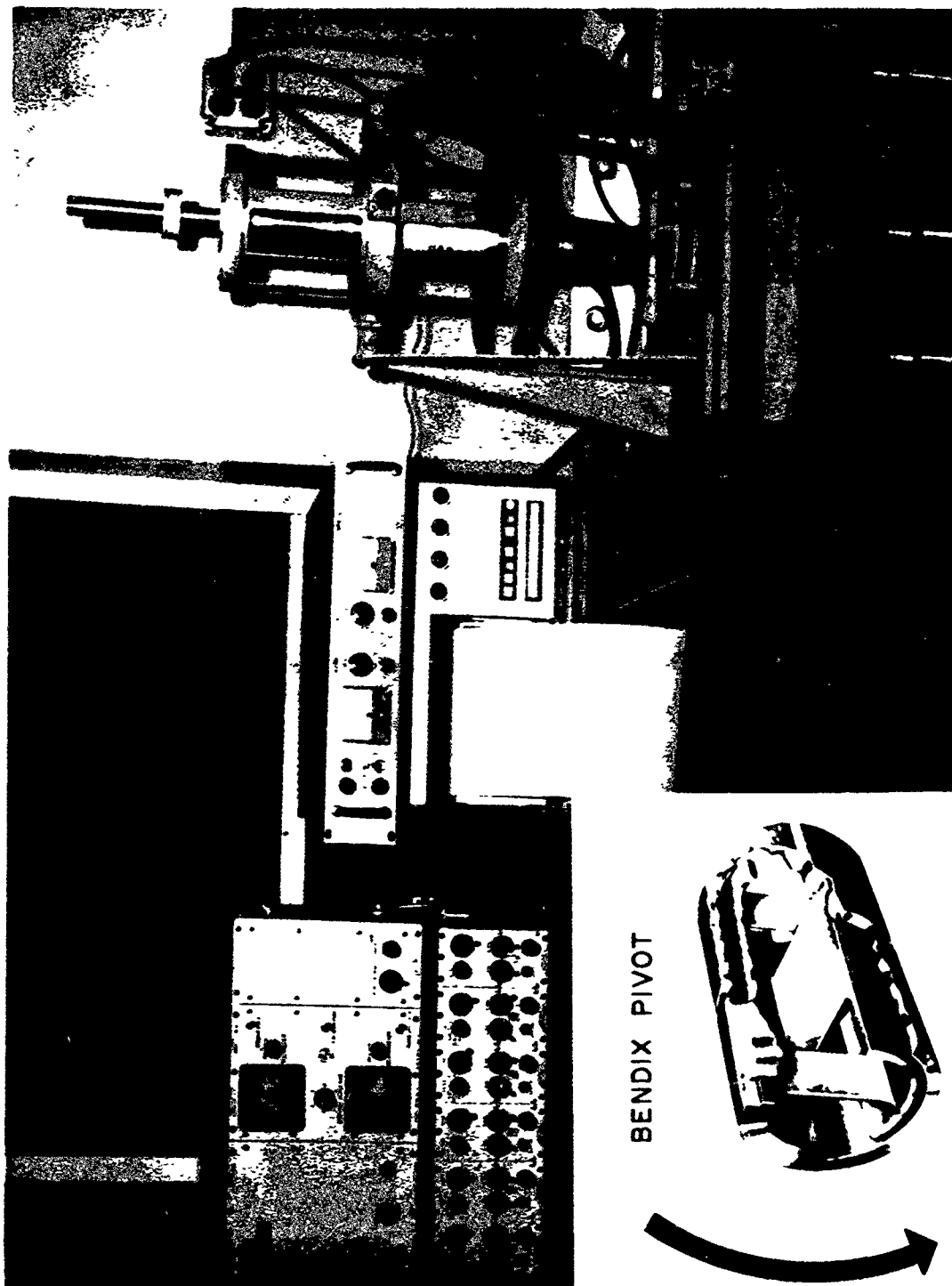
The old gyroscope was described in Reference 1. The new gyroscope is shown in Figure 1. Its principal characteristic is that its inner and outer gimbals are supported by "Bendix Flexure Pivots", shown in an insert in Figure 1. The pivot consists of crossed flexible spring leaves so arranged and mounted that one half of the unit can rotate about the common axis with very little transverse displacement due to the imposed curvature of the springs. The rotation is frictionless, has negligible hysteresis, and is linear (within 2.5 percent) with applied torque up to deflections of 15 degrees.

To measure angular displacement of the gyroscope, strain gages were mounted on one of the pivot spring leaves of the outer gimbal. The strain gages formed part of a bridge circuit whose amplified output was continuously monitored on a photographic recorder provided with calibrated timing lines. Two typical records are shown in Figure 2. Repeatable records could be obtained of oscillations of less than one half degree amplitude.

The rotor is spun by a 27 volt DC motor capable, depending on the load, of spins up to about 7,000 rpm. The spin is controlled by a variable power supply and is measured by a calibrated Strobotac. Two different rotors were constructed, one of steel, another of aluminum. The rotor could accommodate lucite inserts permitting easy construction of cavities of various dimensions and geometries.

The inertial properties of the gyroscope could be varied by additions of heavy brass rings, centered at the pivot point. Thus, the nutational frequency of the system could be changed from $\tau_n = .02$ to $\tau_n = .12$ in increments of .02.

The present experiments were conducted at 5,000 rpm, with cylindrical cavities of diameters of 2 inches and 2.5 inches, and using No. 2 ring. The physical characteristics of the empty gyroscope were:



BENDIX PIVOT

FIG. 1

GYROSCOPE

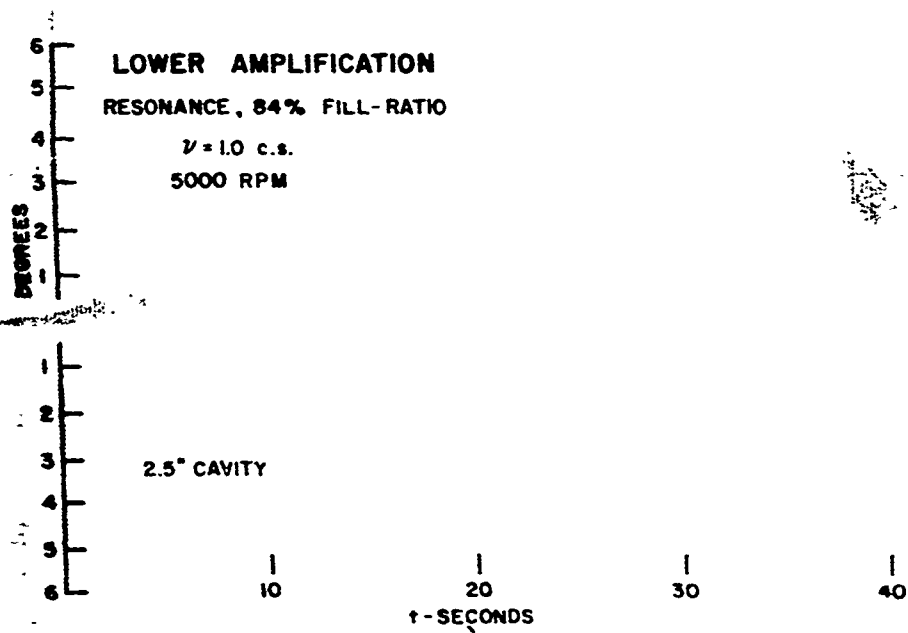
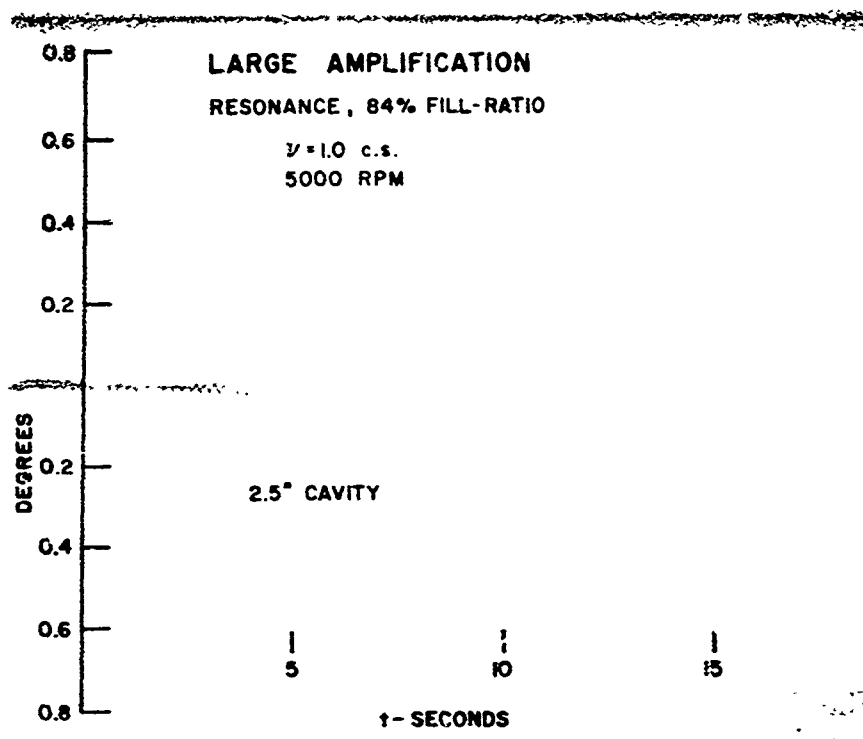


FIG. 2

AMPLITUDE RECORDS

Moments of Inertia, lbs. -in ²	<u>No Fluid</u>	
	2" Cavity	2.5" Cavity
Axial, I_x	82.60	67.25
Transverse, I	1376.7	1260.1
τ_n	.0600	.0534

3. THE EXPERIMENTS

In earlier experiments¹, three liquids were tested: water, $\nu = 1$ c.s.; oil, $\nu = 10$ c.s.; and glycerine, $\nu = 1,000$ c.s.. These tests were supplemented by the data from free-flight tests with 20mm shell using glycerine as a fluid. In the present experiments, silicon oils (Dow Corning Corp.) of various viscosities were used. Table I summarizes pertinent physical characteristics of these oils together with the Reynolds numbers of corresponding experiments.

Table I
Oils and Reynolds Numbers

Viscosity ν , c.s.	Sp. Gr. at 77°F.	Re 2" Cavity	2.5" Cavity
1	.818	3.38×10^5	5.19×10^5
3	.900	1.13×10^5	1.73×10^5
5	.920	6.76×10^4	1.04×10^5
13*	.940	2.60×10^4	4.00×10^4
49*	.960	7.53×10^3	1.06×10^4
100	.958	3.38×10^3	5.19×10^3
350	.972	0.97×10^3	1.48×10^3
1,000	.972	3.38×10^2	5.19×10^2

* Inadvertently, these two oils were partially mixed resulting in above viscosities. Original viscosities were 10 and 50 centistokes.

In order to observe a complete resonance curve, the cavities were designed to resonate at 85 percent fill-ratio. From Stewartson's Tables^{2,4} one finds the required fineness ratio, c/a . For a rotor with 2" cavity diameter, $\tau_n = .060$, the required fineness ratios are:

$$c/a = 1.0307 (2j + 1) \quad j = 0, 1, 2, \dots$$

The chosen cavity was $c/a = 3.092$ ($j = 1$) which had a volume of 328 cc. For a rotor with 2.5" cavity diameter, $\tau_n = .053$.

$$c/a = 1.0257 (2j + 1) \quad j = 0, 1, 2, \dots$$

The chosen cavity was $c/a = 3.077$ ($j = 1$) with a volume of 605 cc. These were convenient cavity sizes.

For some fluids, complete resonance curves were measured by varying fill-ratios. For others, only the peaks of the resonance curves were established.

4. THE DATA

According to the theory of resonance, i.e., when the fundamental fluid frequency, τ_0 , coincides with the nutational frequency of the system, the amplitude of the nutational component of yaw grows as $e^{\alpha_1 t}$, where α_1 is the growth rate and t is the time. From measurements of the amplitudes as a function of time given by the photographic recorder, the rate of divergence is readily established. Table II summarizes these results. A fill-ratio at which the maximum rate of divergence occurs is also included together with the inviscid fundamental fluid frequency corresponding to this fill-ratio.

Two effects of viscosity show clearly in Table II. As viscosity increases, (1) the maximum rate of divergence, at resonance, decreases, (2) maximum instability occurs at progressively higher fill-ratios, or at lower fluid frequencies.

TABLE II

MAXIMUM RATE OF DIVERGENCE OF THE NUTATIONAL AMPLITUDE AT RESONANCE
CORRESPONDING FILL-RATIO AND FUNDAMENTAL FLUID FREQUENCY, τ_{∞} (INVISCID)

Viscosity v c.s.	2" Cavity			2.5" Cavity		
	α_1 per sec	percent	τ_{∞}	α_1 per sec	percent	τ_{∞}
1	.232	83.9	.060	.522	84.5	.055
3	.174	83.9	.060	.431	83.9	.056
5	.138	83.8	.061	.355	84.5	.055
13	.091	84.4	.059	.295	85.1	.053
49	.046	85.5	.055	.160	85.8	.051
100	.040	87.2	.051	.109	86.8	.048
350				.048	88.8	.043
1,000				.029	90.1	.039
τ_n			.060			.055

5. DAMPING FACTORS

As previously pointed out, in the vicinity of resonance the nutational amplitude grows as

$$e^{\alpha_1 t} \quad (\alpha_1 \equiv \omega \tau)$$

where ω is the axial spin of the gyroscope and

$$\tau = 1/2 \sqrt{S - (\tau_o - \tau_n)^2} \quad (1)$$

$$S = \frac{\rho a^5 (2R)^2}{I_x \sigma c/a}$$

ρ = fluid density,

a = radius of the cavity,

2R = tabulated function in Stewartson Tables,
 [Note: In Reference 2 this is called R,
 but a factor of 4 is missing in the Equation
 (5.12). In Reference 4, 2R is tabulated.
 Numerically, however, the two tables are
 identical],

$$\sigma = \sqrt{1 - 1/s}, \quad s = \text{gyroscopic stability factor,}$$

$$I_x = \text{polar moment of inertia,}$$

$$c/a = \text{fineness ratio of the cavity.}$$

For instability, τ must be real, or

$$S - (\tau_o - \tau_n)^2 > 0. \quad (2)$$

The maximum rate of divergence is at exact resonance, $\tau_o = \tau_n$, for which the inviscid rate of divergence is:

$$(\alpha_1)_i = \omega \tau_i = \frac{\omega}{2} \sqrt{S} \quad (3)$$

where τ_i is the inviscid τ as given by Stewartson's theory. Since \sqrt{S} is essentially a constant, inviscid theory does not account for the observed behavior of $(\alpha_1)_{\max}$ for various fluids as shown in Table II.

In Reference 1 it is shown that a marked improvement in the agreement between the theory and the observations can be achieved by making the eigen frequencies of the fluid complex quantities, i.e., introducing a damping factor. As shown by Wedemeyer³, the damping factor arises as a natural consequence of the existence of the boundary layer on the walls of the cavity acting as an energy sink. If one modifies Stewartson's frequencies by adding an imaginary component.

$$\tau_o = \tau_{oo} + i\delta \quad (4)$$

it can be easily shown¹ that an expression for the viscous τ , τ_v , becomes:

$$\tau_v = 1/2 \left[\sqrt{\frac{m + \sqrt{m^2 + n^2}}{2}} - \delta \right] \quad (5)$$

where

$$m \equiv S + \delta^2 - (\tau_{oo} - \tau_n)^2$$

$$n \equiv 2\delta(\tau_{oo} - \tau_n) \quad .$$

At resonance, $\tau_{oo} - \tau_n = 0$, Equation (5) simplifies to

$$\tau_v = 1/2 \left[\sqrt{S + \delta^2} - \delta \right] \quad . \quad (6)$$

The maximum viscous divergence rate is:

$$(\alpha_1)_v = \omega \tau_v \quad .$$

We assume that the observed maximum divergence rates, Table II, are viscous rates, i.e.:

$$(\alpha_1)_{obs} \equiv (\alpha_1)_v \quad .$$

To determine δ , the damping factor, we form a ratio of the theoretical inviscid to viscous rates at resonance

$$r = \frac{(\alpha_1)_i}{(\alpha_1)_v} = \frac{\tau_i}{\tau_v} = \frac{\sqrt{S}}{\sqrt{S + \delta^2} - \delta} \quad (7)$$

and use the above assumption. From Equation (7):

$$\delta = 1/2 \sqrt{S} \left(r - \frac{1}{r} \right) \quad . \quad (8)$$

Table III summarizes the damping factors so computed together with other pertinent information.

TABLE III

v c.s.	2" Cavity			2.5" Cavity				
	\sqrt{S} x 10 ³	(α_1) _i per sec	(α_1) _v Table II	δ x 10 ³	\sqrt{S} x 10 ³	(α_1) _i per sec	(α_1) _v Table II	δ x 10 ³
1	1.89	.495	.232	1.57	3.19	.836	.522	1.56
3	1.98	.518	.174	2.61	3.35	.877	.431	2.59
5	2.01	.526	.138	3.57	3.39	.887	.355	3.56
13	2.03	.531	.091	5.75	3.43	.897	.295	4.65
49	2.05	.537	.046	11.88	3.46	.907	.160	9.51
100	2.06	.539	.040	13.80	3.48	.911	.109	14.33
350	2.06	.539			3.48	.912	.048	33.01
1000	2.06	.539			3.48	.912	.029	54.73

A plot of $\log \delta$ vs $\log Re$ (Table I) is shown in Figure 3. As can be seen, a slope of $-1/2$ satisfies the observations reasonably well. With these data it is found that the damping factor, for $j = 1$ mode, can be represented by

$$\delta = \frac{1.04 \pm .12 \text{ s.d.}}{\sqrt{Re}} \quad (9)$$

Figures 4 and 5 show a comparison between the observed and the theoretically computed resonance curves for two oils, $\nu = 1$ c.s. and $\nu = 100$ c.s. Theoretical curves were computed using Equation (5) with the damping factor as given by Equation (9). The agreement is quite good although for the more viscous oil the width of the resonance band is somewhat overestimated. From Table III, the inviscid heights of the α_1 vs τ curves are 1.7 and 8.4 times the viscous heights for the two oils, respectively. The inviscid half width of the resonance curve is .003 on the τ scale. Therefore, the differences between the viscous and the inviscid resonance curves are quite large, especially for more viscous oils.

Figure 3 also shows the data from Reference 1. These observations, as reported, are reasonably well represented by

$$\delta = \frac{.14 \pm .02 \text{ s.d.}}{\sqrt[4]{Re}} \quad (10)$$

As previously surmised, the difference between Equations (9) and (10) might be due to change in the character of the boundary layer at larger amplitudes (data of Reference 1). The change in the boundary layer may alter the rate at which the nutational amplitude grows and, hence, the inferred damping factor.

6. THE AMPLITUDES

As designed, the limiting amplitude of oscillations of the present gyroscope is 15° . This limit is imposed by the Bendix pivots and the gyroscope is provided with a suitable amplitude limiting ring, see

DAMPING FACTORS VS R_0

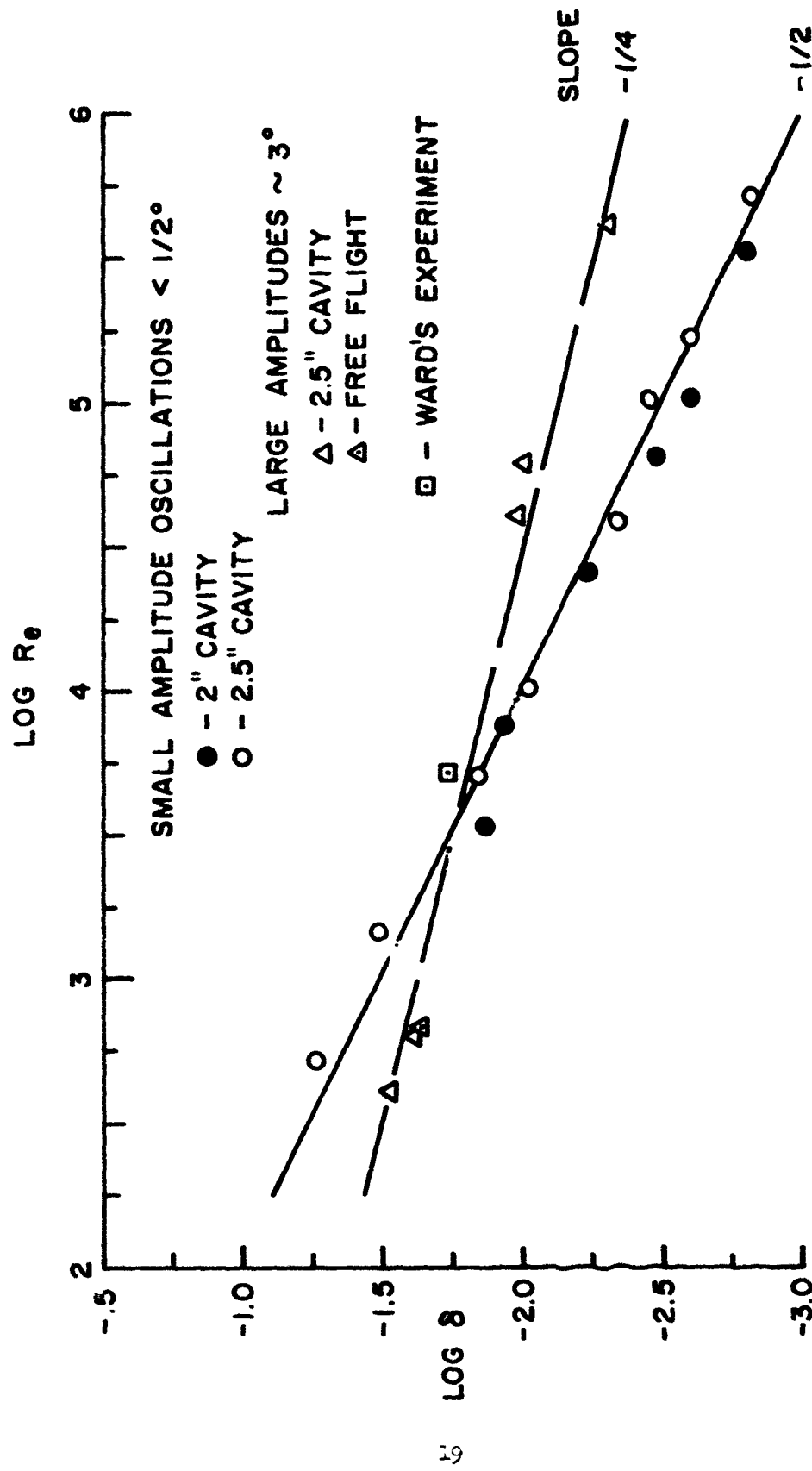
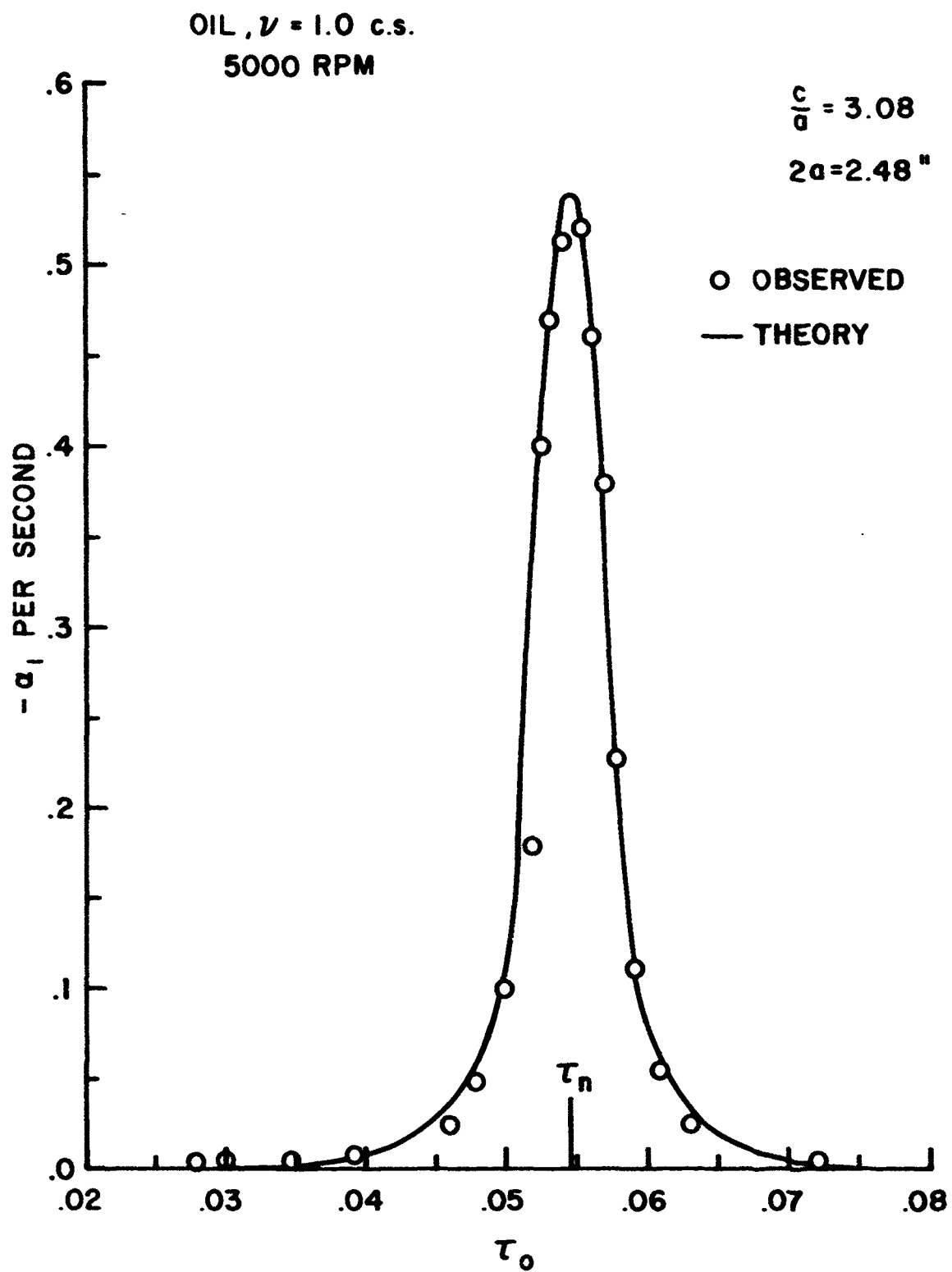


FIG. 3

RATE OF DIVERGENCE vs τ , $\nu = 1 \text{ c.s.}$



RATE OF DIVERGENCE vs τ , $\nu = 100$ c.s.

OIL, $\nu = 100$ c.s.
5000 RPM

$$\frac{c}{a} = 3.08$$

$$2a = 2.48''$$

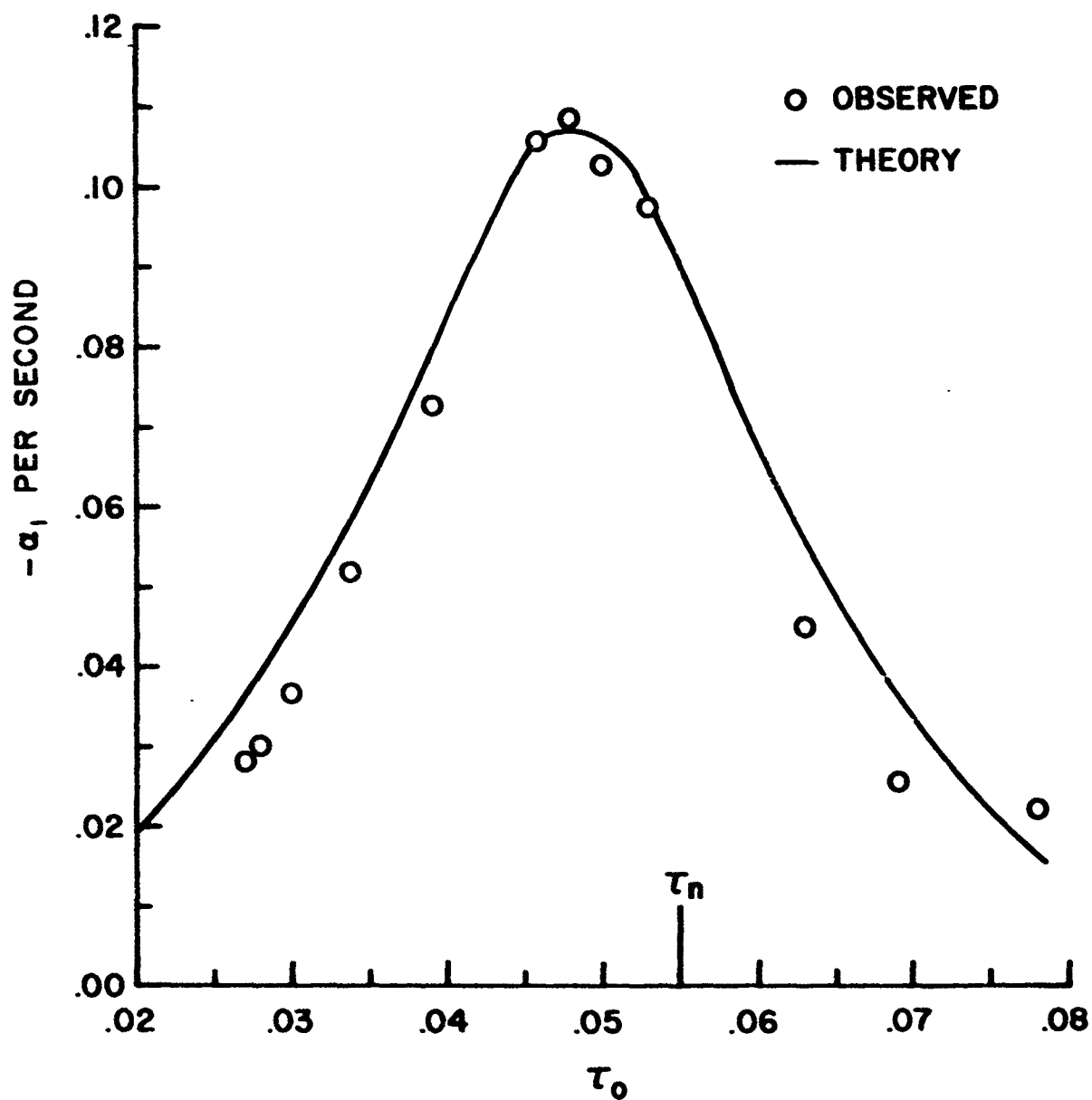


FIG. 5

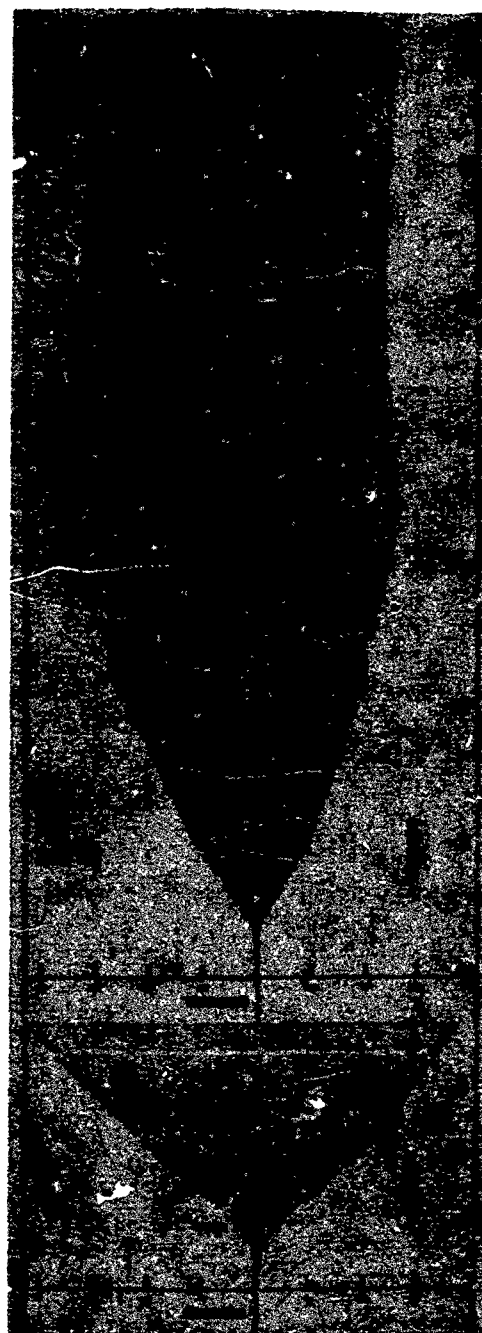
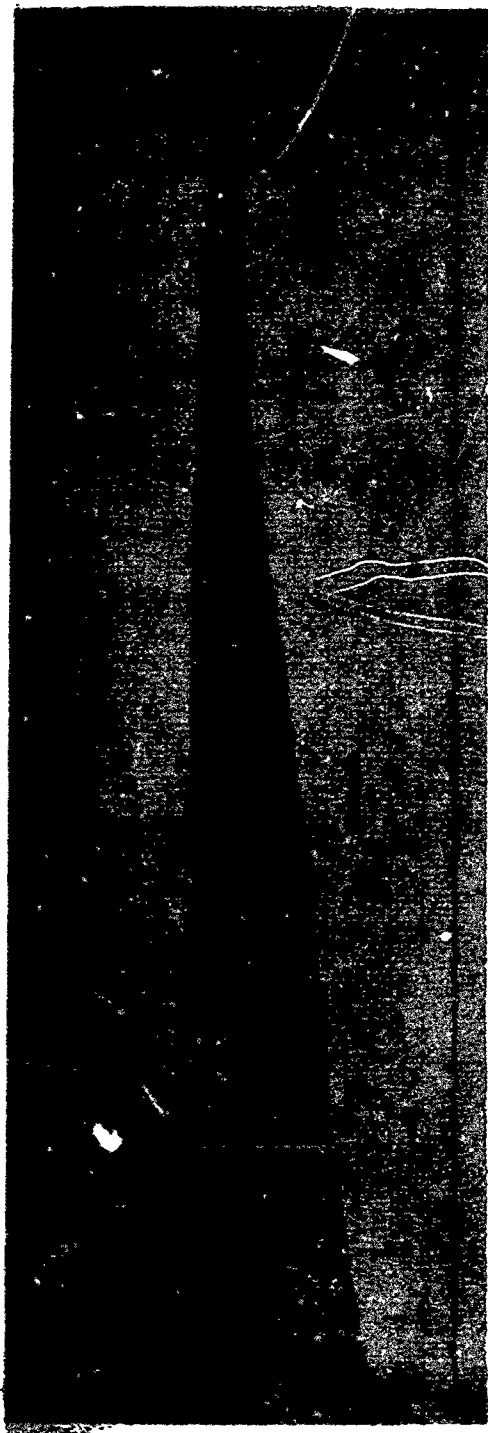
Figure 1. In practice, however, because of slight precessional motion, due to very small asymmetries present in the system, the maximum unrestricted amplitude was found to be only 12° .

A series of amplitude records, at exact resonance, with the gyroscope empty and filled with oils of various viscosities are shown in Figures 6, 7, 8, and 9. The vertical grid lines are one second intervals. The origin of the specially marked time scale is arbitrary. The discontinuities in the records are special timing marks of the recorder.

The records show a number of interesting features. Initially, the amplitude grows exponentially, and the rates given in Table II correspond to this growth. This rate, however, suffers a rather sudden discontinuity, see Figure 2. Following this discontinuity, the amplitude maintains, for awhile, its exponential growth, but at a new rate. As amplitude continues to grow, there appear other breaks and wrinkles in the envelopes of amplitudes for lighter oils. But, on the whole, beyond a certain level of amplitude, the amplitude grows more nearly linearly rather than exponentially. Finally, by a rather sharp break, the amplitude reaches a constant value and ceases to grow further, see Figures 6 and 7. This appears to be a steady state condition for, in some experiments, the gyroscope was permitted to run for as long as twelve minutes with the amplitude remaining at an essentially constant value. At larger viscosities, the level of constant amplitude increases. For the most viscous oils, the constant amplitude plateau was beyond the reach of the gyroscope with its limiting amplitude of 12° , see Figure 9.

It is probable that, at lower amplitudes, the breaks in the rate of growth are associated with the changes in the character of the boundary layer; as the amplitude grows, non-linear effects become progressively more important.

For low viscosity oils, i.e., high Reynolds numbers, the first discontinuity in the rate occurs at rather small amplitudes, see Figure 2. However, this discontinuity is progressively delayed as the viscosity increases. The first break is marked by an arrow on the records and the



AMPLITUDES: EMPTY GYROSCOPE AND WITH OIL, $\nu = 1$ c.s. FIG. 6

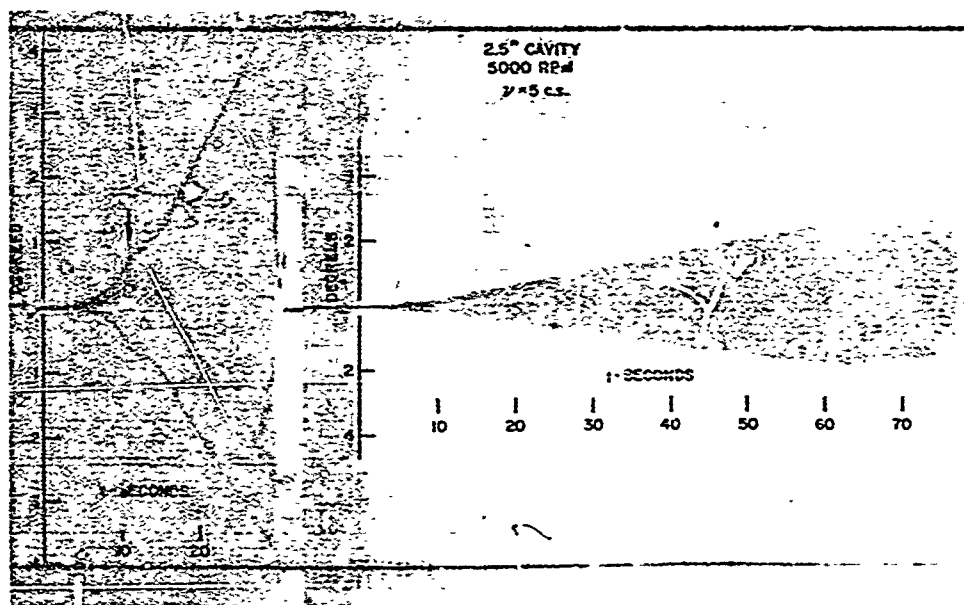
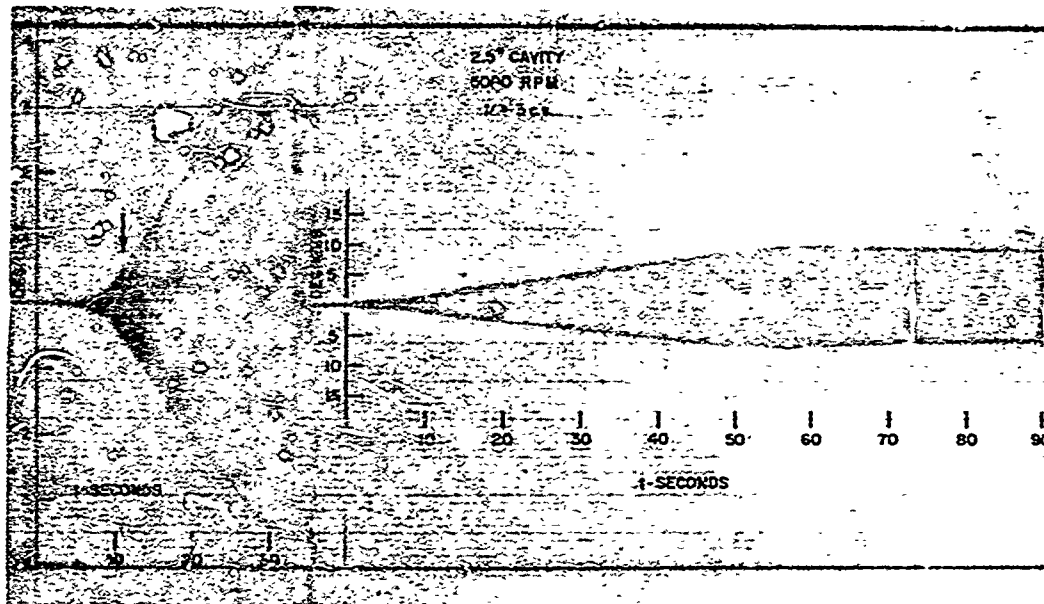


FIG. 7

AMPLITUDES: $v = 3$ c.s., and $v = 5$ c.s.

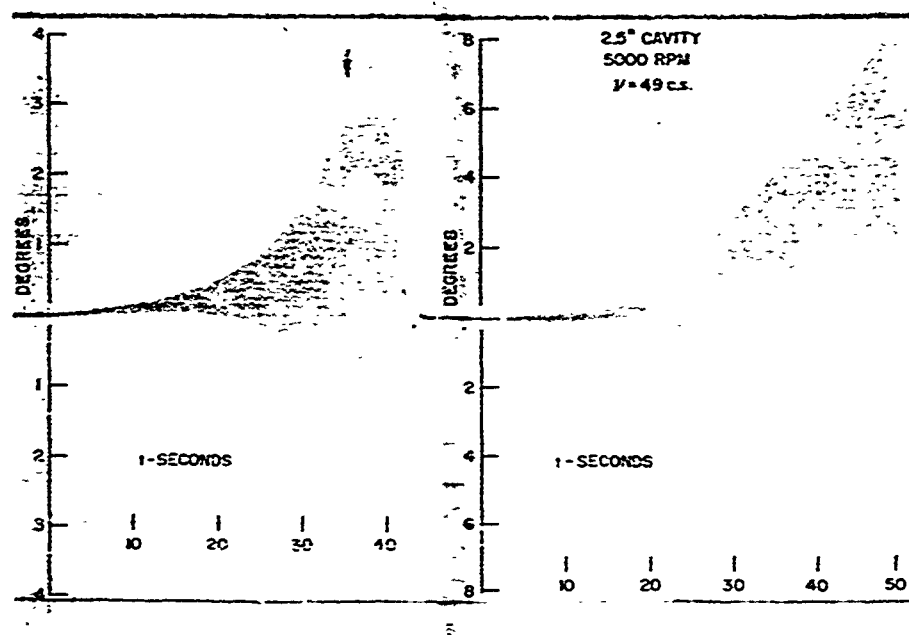
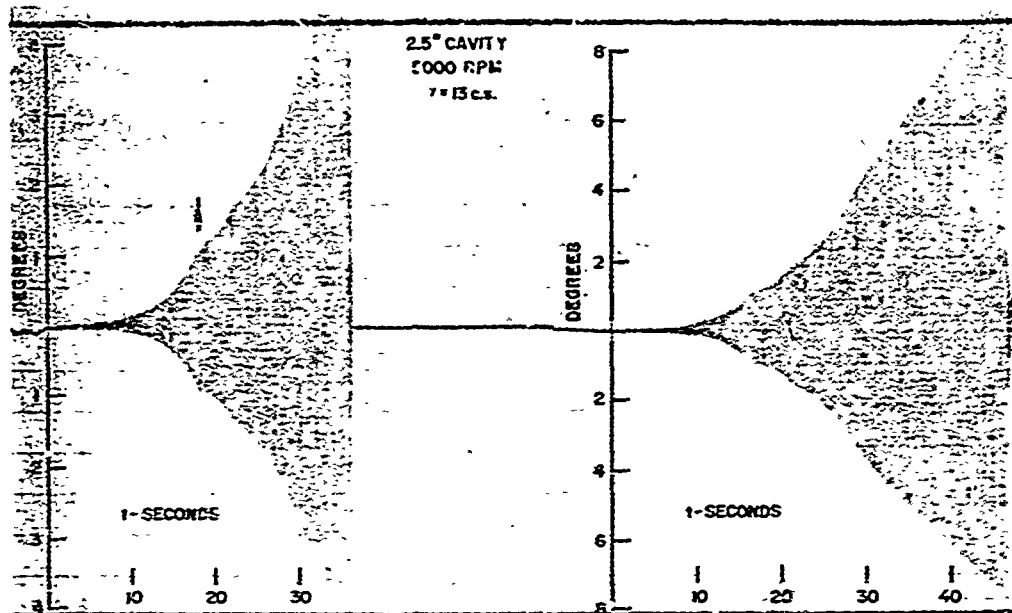


FIG. 8

AMPLITUDES: $\nu = 13$ c.s., and $\nu = 49$ c.s.

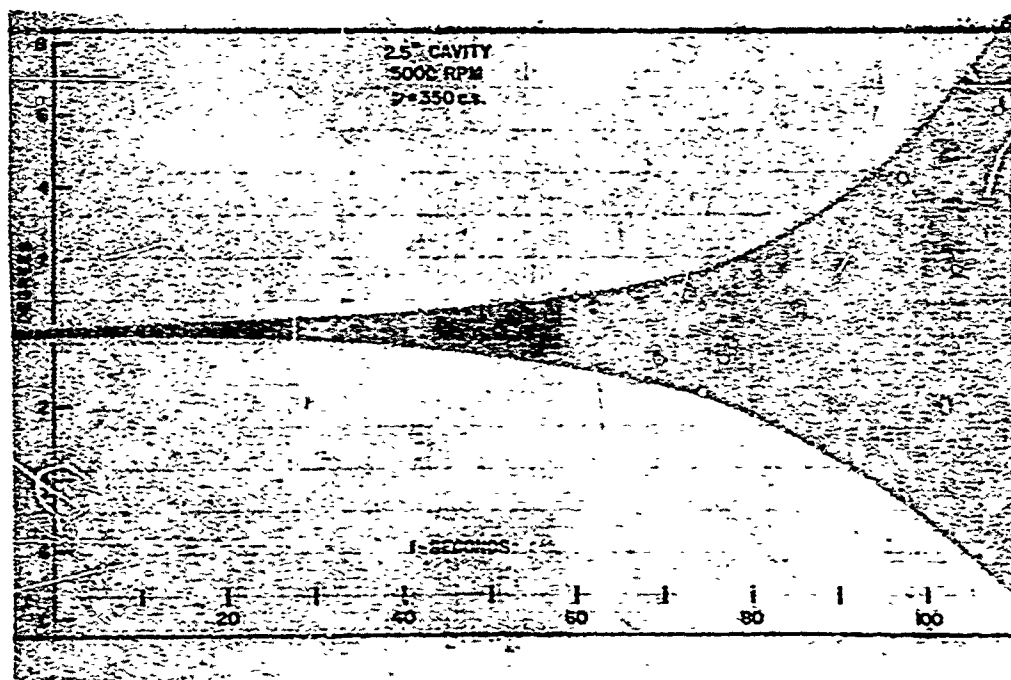
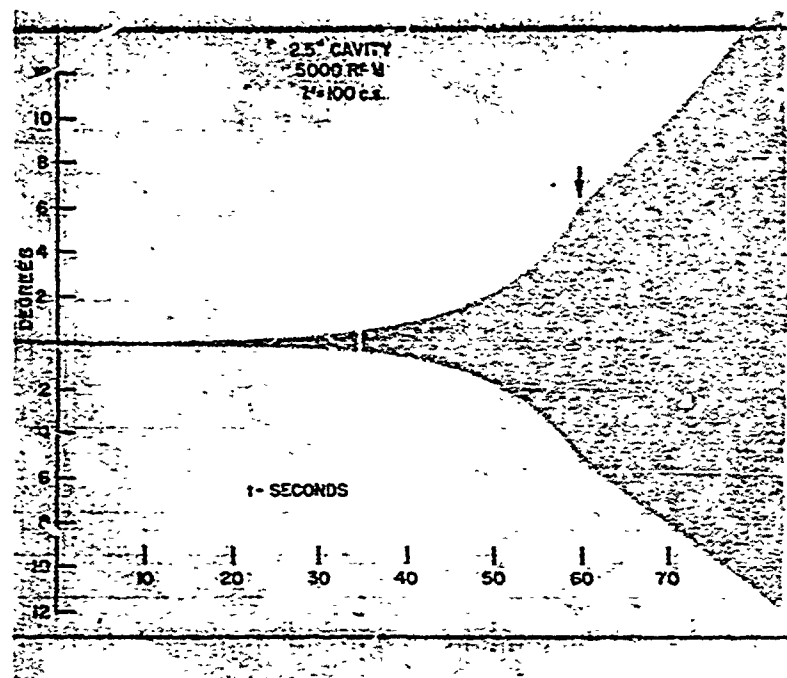


FIG 9

AMPLITUDES: $\nu = 100$ c.s., and $\nu = 350$ c.s.

approximate amplitude at which it occurs is given in the following table:

ν c.s.	Amplitude, degrees
1	.5
3	.7
5	.75
13	1.0
49	2.6
100	5.5

A semi-log plot of the amplitude vs time for $\nu = 1$ c.s. in the 2.5" cavity is given in Figure 10. This is to be regarded only as an illustration of a general trend, with small irregularities removed. Similar plots for various viscosity oils tested in the 2" cavity are shown in Figure 11. The effect of spin on growth of amplitude in the 2" cavity is shown in Figure 12. It is to be noted that the constant amplitude level is more sensitive to the diameter of the cavity than to the spin.

As shown by the records, and the graphs, the rate of growth of the amplitude is amplitude dependent. The damping factor, therefore, is also amplitude dependent since it is related to the ratio of the inviscid to viscous rates, and the inviscid rate is assumed constant. Hence, care must be exercised in assigning physical significance to the exponent of Re obtained from the correlation of the damping factor with the Reynolds numbers. At very small amplitudes the exponential rate is amplitude independent, and the exponent of Re probably has the physical significance assigned to it, that is, that the boundary layer is laminar.

To illustrate the dependence of damping factors on amplitude, damping factors were computed from measured rates at three points on amplitude curves: just following the first discontinuity, and at 2° and 4° . The results are shown in Figure 13. The two lines, transposed from Figure 3, with slopes of $-1/2$ and $-1/4$, do satisfy some of these observations: the $-1/2$ line for heavier oils at all three amplitudes, and $-1/4$ line for lighter oils at about 1° amplitude. The former reflects the fact that for heavier oils the first discontinuity in the rate occurs at amplitudes larger than 4° .

GROWTH OF AMPLITUDE AT RESONANCE

$V = 1.0$ c.s.

5000 RPM

2.5" CAVITY

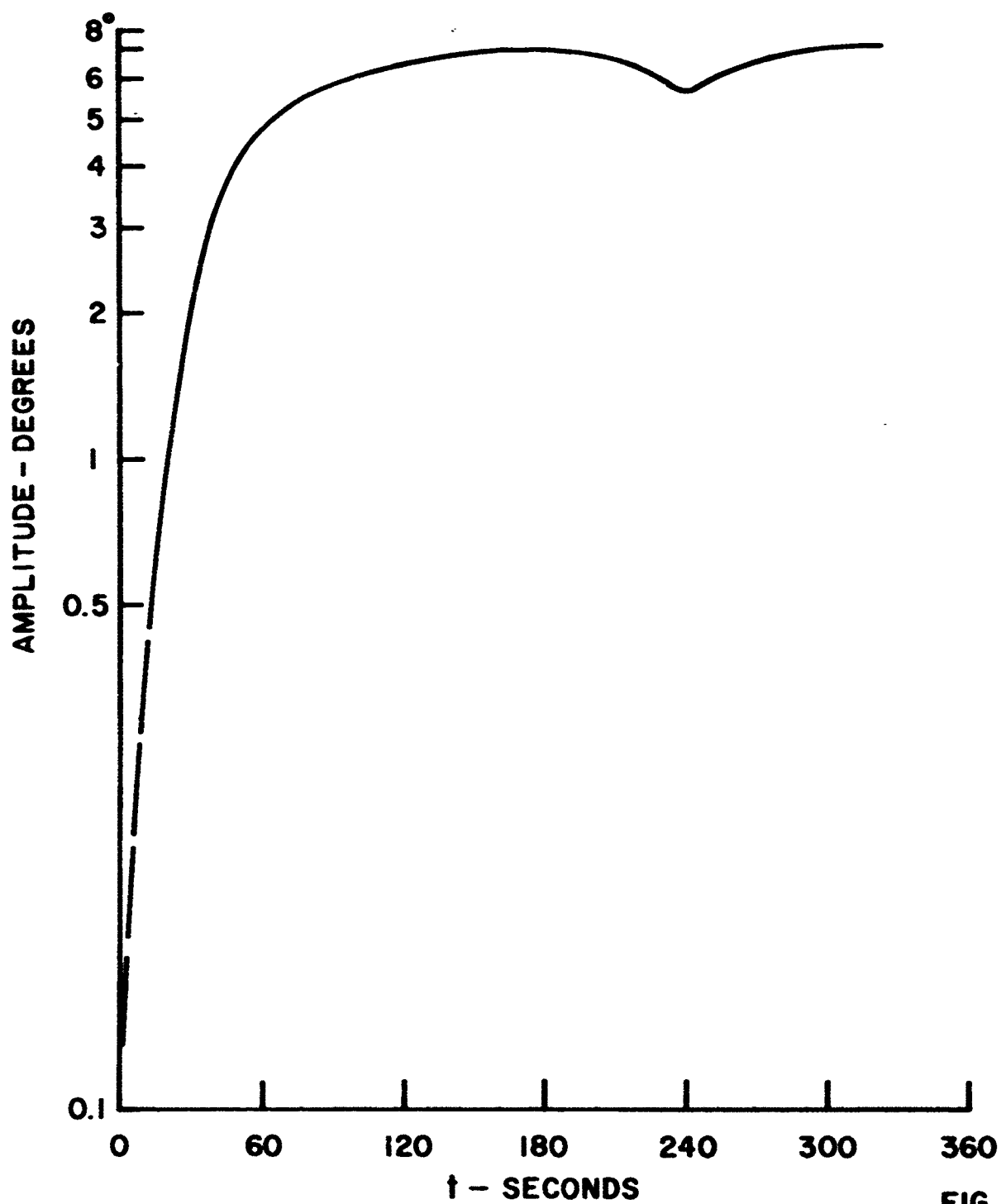


FIG. 10

GROWTH OF AMPLITUDE AT RESONANCE FOR VARIOUS VISCOSITIES

2" CAVITY

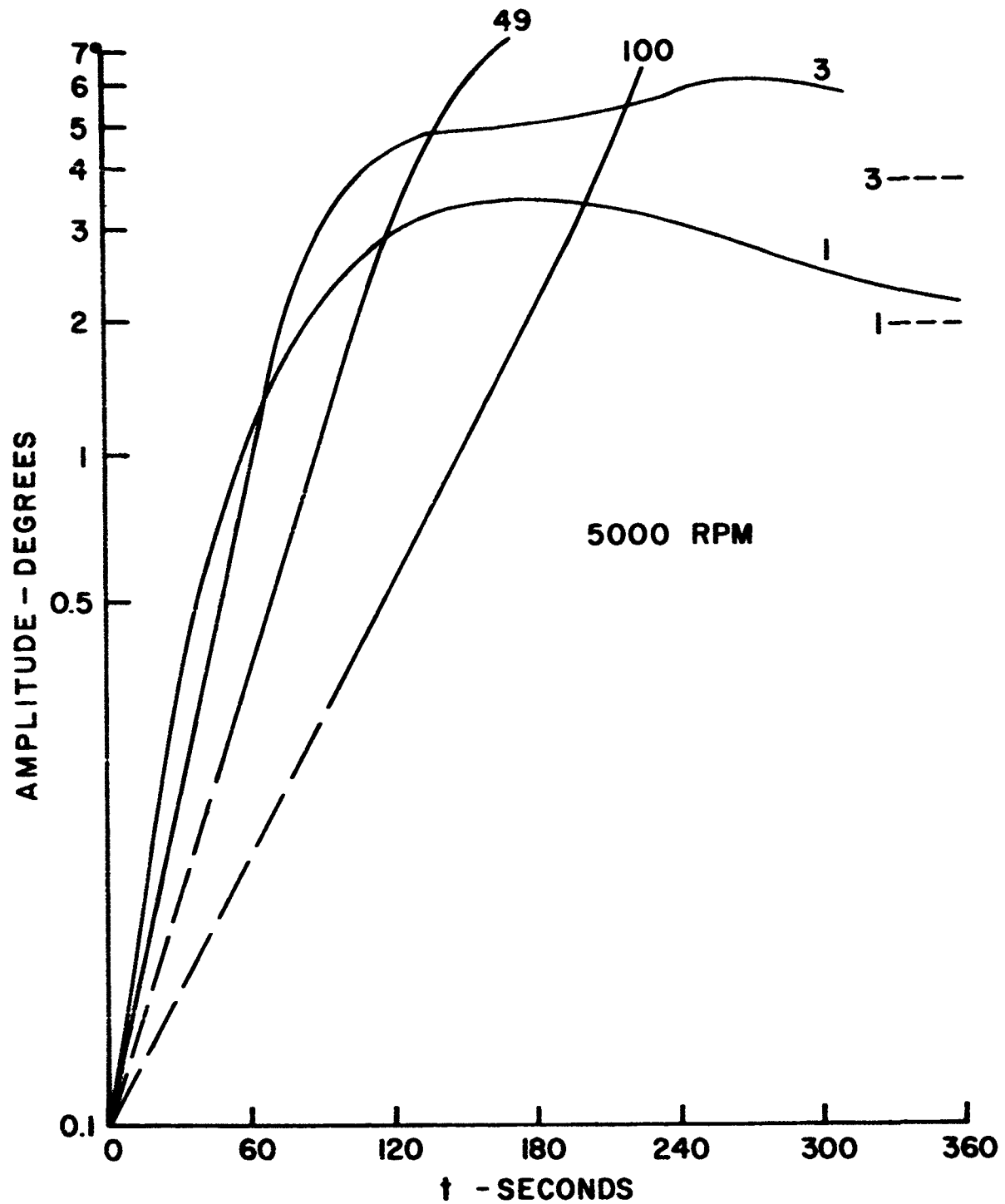
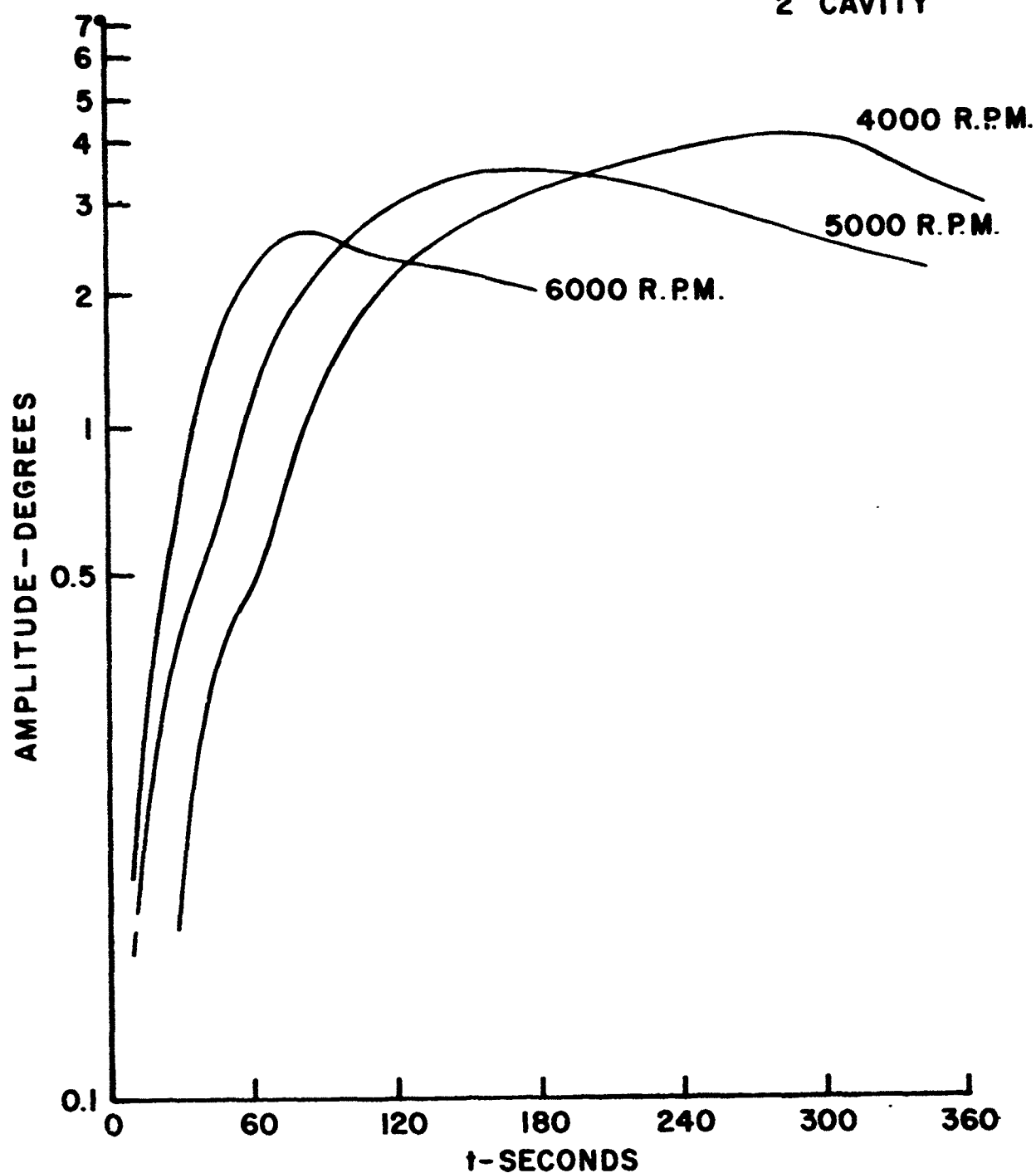


FIG. II

GROWTH OF AMPLITUDE AT RESONANCE FOR VARIOUS SPIN RATES

$\nu = 1 \text{ c.s.}$

2" CAVITY



DAMPING FACTORS VS R_e AT VARIOUS AMPLITUDES

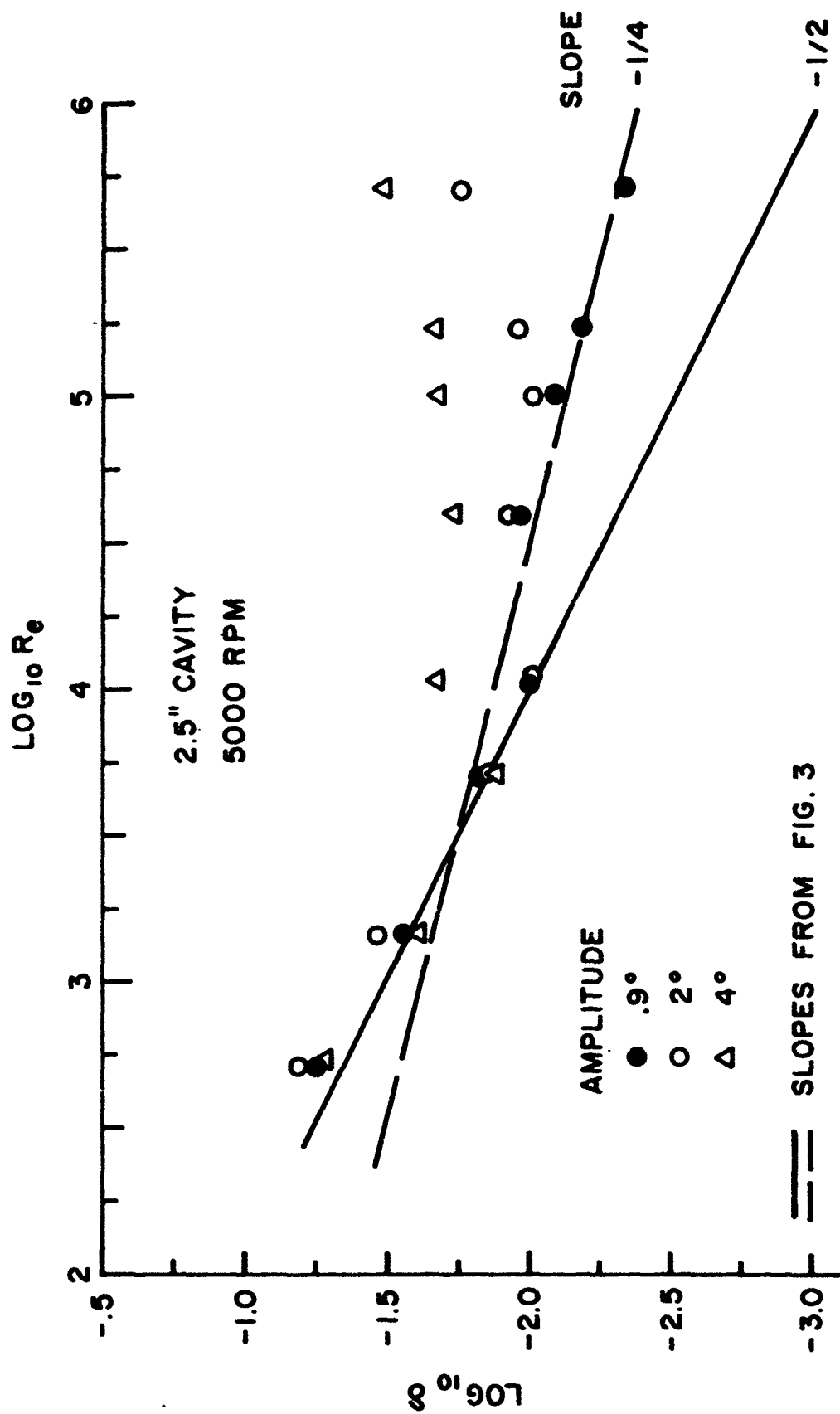


FIG. 13

For lighter oils ($\nu = 1, 3, 5$, and 13 centistokes), although the damping factors at one degree amplitude seem to lie close to the $-1/4$ line, there is a systematic trend with viscosity away from this line. The data for these four oils are better represented by

$$\delta = \frac{.38}{\sqrt[3]{Re}} \quad (11)$$

Whether such dependence of δ on Re is also fortuitous, as is the $-1/4$ power obtained in Reference 1, or has some physical significance in terms of the nature of the boundary layer, at present is unknown.

7. FREQUENCY DISPLACEMENT

Table II shows that there is a progressive shift in the resonant fluid frequency with viscosity. The shift arises from slight change in the effective fineness ratio of the cavity due to presence of the boundary layer. The theory³ shows that this displacement is a similar function of the Reynolds numbers as is the amplitude at resonance, i.e.

$$\Delta\tau = \tau_{oo} - \tau_n = \frac{\text{constant}}{\sqrt{Re}} \quad (12)$$

Present data, at small amplitudes, is consistent with this prediction as is shown in Figure 14. Because of the uncertainty of the small displacement at lower viscosities, especially when plotted on logarithmic scale, only $\Delta\tau$'s for $\nu \geq 13$ c.s. are included. Also are included data from Reference 1. The observed displacement is reasonably well represented by

$$\Delta\tau = \tau_{oo} - \tau_n = - \frac{.41 \pm .06 \text{ s.d.}}{\sqrt{Re}} \quad (13)$$

where τ_{oo} is the inviscid frequency. Therefore, in a cylindrical cavity with a fineness ratio, $c/a \approx 3$, the maximum instability occurs at an inviscid fluid frequency

$$(\tau_{oo})_{\max} = \tau_n - \frac{.41}{\sqrt{Re}} \quad (14)$$

DISPLACEMENT $\Delta \tau$ VS R_e

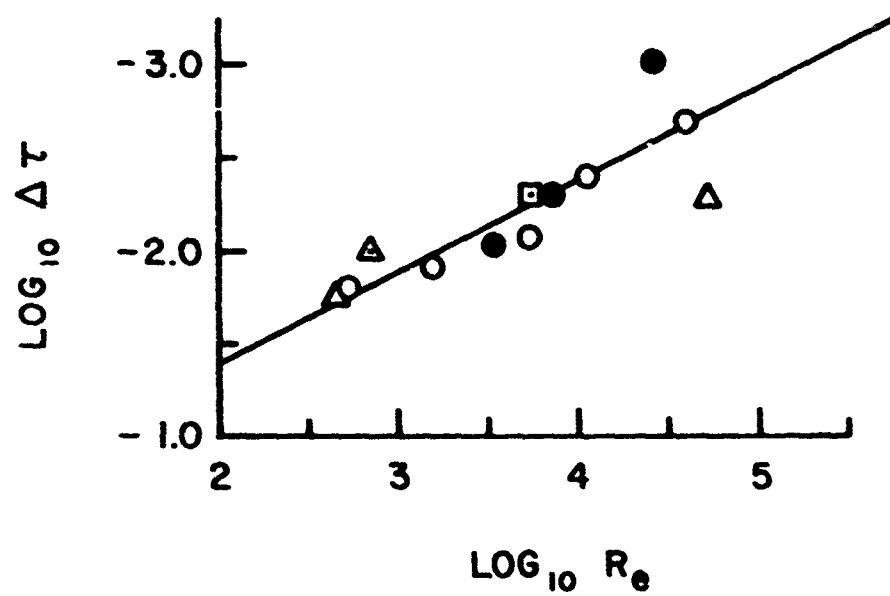
SMALL AMPLITUDES

- - 2" CAVITY
- - 2.5" CAVITY

LARGE AMPLITUDES

- △ - 2.5" CAVITY
- △ - FREE FLIGHT

□ WARD'S EXPERIMENT



and not at $\tau_{00} = \tau_n$. In other words, the maximum instability occurs either at slightly higher fill-ratio or smaller fineness ratio than those predicted by the inviscid theory. For other modes, the constant in Equation (14) might be different.

8. CONCLUDING REMARKS

It has been demonstrated that Stewartson's inviscid theory of resonance, with Wedemeyer's viscous correction, gives excellent predictions over a wide range of Reynolds numbers of the fill-ratio at which the resonance occurs. Moreover, it accurately predicts the initial rate of growth of the nutational component at resonance. In practice, such information should be of great value to designers of liquid filled shell configurations. However, demonstrated nonlinear or amplitude dependent behavior should be kept in mind.

The following illustrates the consequences of nonlinear behavior which may lead the designer astray. The 2.5" cavity was completely filled with $\nu = 1$ c.s. oil. According to Figure 4, at 100 percent full, $\tau_0 = .028$, the gyroscope is practically stable, i.e., $\alpha_1 \approx 0$. Experiments were performed with several arbitrarily imposed different initial amplitudes. Up to about six degrees the amplitude showed essentially zero damping. Above this amplitude, the amplitude suddenly diverged reaching a constant level of ten degrees. In practice, therefore, the shell may be designed to be stable at small launch yaws and, yet, develop "sudden" instability at summittal yaws. Such behaviors were apparently encountered in practice, i.e., dependence of behavior on quadrant elevation.

Long ordnance experience with liquid filled shell led to the recognition of several variables which appeared to influence their dynamics. These are:

1. Air space in cavity
2. Specific gravity of the liquid
3. Liquid viscosity
4. Spin level of the shell

5. Shell velocity
6. Quadrant elevation
7. Geometry of the cavity.

For cylindrical cavities, Stewartson's inviscid theory with Wedemeyer's viscous correction adequately accounts for the first three variables. The next three are probably related to non-linear behavior of the oscillating fluid at larger amplitudes. The last item needs further investigation.

B. G. KARPOV

REFERENCES

1. Karpov, B. G. Dynamics of Liquid Filled Shell: Resonance and Effect of Viscosity. BRL Report No. 1279, May 1965.
2. Stewartson, K. On the Stability of a Spinning Top Containing Liquid. J. Fluid Mech, 5, Part 4, 1959.
3. Wedemeyer, E. H. Dynamics of Liquid Filled Shell: Theory of Viscous Corrections to Stewartson Stability Problem. BRL Report No. 1287, June 1965.
4. Karpov, B. G. Dynamics of Liquid Filled Shell: Aids for Designers. BRL Memorandum Report No. 1477, May 1963.

Unclassified
Security Classification

DOCUMENT CONTROL DATA - R&D		
(Security classification of title, body of abstract and indexing annotation must be entered when the overall report is classified)		
1. ORIGINATING ACTIVITY (Corporate author) U. S. Army Ballistic Research Laboratories Aberdeen Proving Ground, Maryland		2a. REPORT SECURITY CLASSIFICATION Unclassified
		2b. GROUP
3. REPORT TITLE LIQUID FILLED GYROSCOPE: THE EFFECT OF REYNOLDS NUMBER ON RESONANCE		
4. DESCRIPTIVE NOTES (Type of report and inclusive dates)		
5. AUTHOR(S) (Last name, first name, initial) Karpov, Boris G.		
6. REPORT DATE October 1965	7a. TOTAL NO. OF PAGES 41	7b. NO. OF REFS 4
8a. CONTRACT OR GRANT NO.	9a. ORIGINATOR'S REPORT NUMBER(S) Report No. 1302	
b. PROJECT NO. 1P014501A33D		
c.	9b. OTHER REPORT NO(S) (Any other numbers that may be assigned this report)	
d.		
10. AVAILABILITY/LIMITATION NOTICES This document is subject to special export controls and each transmittal to foreign governments or foreign nationals may be made only with prior approval of U.S. Army Materiel Command, Attn: AMCMU-IS, Washington, D.C.		
11. SUPPLEMENTARY NOTES	12. SPONSORING MILITARY ACTIVITY U. S. Army Materiel Command Washington, D. C.	
13. ABSTRACT A gyroscope with frictionless bearings was designed and built. Resonance experiments with oils of various viscosities substantiated the results of the authors previous work, i.e., to account for the observed behavior of the gyroscope at resonance, Stewartson's inviscid theory requires a viscous correction. Wademyer's theory for viscous correction predicts that, for a laminar boundary layer on the walls of the cavity, the damping factor should be of the form $\delta = \frac{\text{constant}}{\sqrt{Re}}$ This has been verified by present experiments. The experiments also showed that the rate of growth of the nutational amplitude at resonance is strongly influenced by the nature of the boundary layer. At larger amplitudes, non-linear behavior of the oscillating fluid appears to dominate responses of the gyroscope.		

DD FORM 1473
1 JAN 64

Unclassified
Security Classification

1a. KEY WORDS	LINK A		LINK B		LINK C	
	ROLE	WT	ROLE	WT	ROLE	WT
Dynamics Liquid-Filled Shell Flight Mechanics Gyroscopes						

INSTRUCTIONS

1. **ORIGINATING ACTIVITY:** Enter the name and address of the contractor, subcontractor, grantee, Department of Defense activity or other organization (*corporate author*) issuing the report.

2a. **REPORT SECURITY CLASSIFICATION:** Enter the overall security classification of the report. Indicate whether "Restricted Data" is included. Marking is to be in accordance with appropriate security regulations.

2b. **GROUP:** Automatic downgrading is specified in DoD Directive 5200.10 and Armed Forces Industrial Manual. Enter the group number. Also, when applicable, show that optional markings have been used for Group 3 and Group 4 as authorized.

3. **REPORT TITLE:** Enter the complete report title in all capital letters. Titles in all cases should be unclassified. If a meaningful title cannot be selected without classification, show title classification in all capitals in parenthesis immediately following the title.

4. **DESCRIPTIVE NOTES:** If appropriate, enter the type of report, e.g., interim, progress, summary, annual, or final. Give the inclusive dates when a specific reporting period is covered.

5. **AUTHOR(S):** Enter the name(s) of author(s) as shown on or in the report. Enter last name, first name, middle initial. If military, show rank and branch of service. The name of the principal author is an absolute minimum requirement.

6. **REPORT DATE:** Enter the date of the report as day, month, year, or month, year. If more than one date appears on the report, use date of publication.

7a. **TOTAL NUMBER OF PAGES:** The total page count should follow normal pagination procedures, i.e., enter the number of pages containing information.

7b. **NUMBER OF REFERENCES:** Enter the total number of references cited in the report.

8a. **CONTRACT OR GRANT NUMBER:** If appropriate, enter the applicable number of the contract or grant under which the report was written.

8b, 8c, & 8d. **PROJECT NUMBER:** Enter the appropriate military department identification, such as project number, subproject number, system numbers, task number, etc.

9a. **ORIGINATOR'S REPORT NUMBER(S):** Enter the official report number by which the document will be identified and controlled by the originating activity. This number must be unique to this report.

9b. **OTHER REPORT NUMBER(S):** If the report has been assigned any other report numbers (*either by the originator or by the sponsor*), also enter this number(s).

10. **AVAILABILITY/LIMITATION NOTICES:** Enter any limitations on further dissemination of the report, other than those imposed by security classification, using standard statements such as:

- (1) "Qualified requesters may obtain copies of this report from DDC."
- (2) "Foreign announcement and dissemination of this report by DDC is not authorized."
- (3) "U. S. Government agencies may obtain copies of this report directly from DDC. Other qualified DDC users shall request through _____."
- (4) "U. S. military agencies may obtain copies of this report directly from DDC. Other qualified users shall request through _____."
- (5) "All distribution of this report is controlled. Qualified DDC users shall request through _____."

If the report has been furnished to the Office of Technical Services, Department of Commerce, for sale to the public, indicate this fact and enter the price, if known.

11. **SUPPLEMENTARY NOTES:** Use for additional explanatory notes.

12. **SPONSORING MILITARY ACTIVITY:** Enter the name of the departmental project office or laboratory sponsoring (*paying for*) the research and development. Include address.

13. **ABSTRACT:** Enter an abstract giving a brief and tactical summary of the document indicative of the report, even though it may also appear elsewhere in the body of the technical report. If additional space is required, a continuation sheet shall be attached.

It is highly desirable that the abstract of classified reports be unclassified. Each paragraph of the abstract shall end with an indication of the military security classification of the information in the paragraph, represented as (TS), (S), (C), or (U).

There is no limitation on the length of the abstract. However, the suggested length is from 150 to 225 words.

14. **KEY WORDS:** Key words are technically meaningful terms or short phrases that characterize a report and may be used as index entries for cataloging the report. Key words must be selected so that no security classification is required. Identifiers, such as equipment model designation, trade name, military project code name, geographic location, may be used as key words but will be followed by an indication of technical context. The assignment of links, rules, and weights is optional.